

Imaging Super Massive Black Holes and the Origin of Jets – Global mm- and sub-mm-VLBI Studies of Compact Radio Sources

A Whitepaper and Proposal for submm-VLBI with APEX and ALMA

T.P. Krichbaum, J.A. Zensus, W. Alef, A. Roy, D. Graham,
K. Menten, R. Güsten, D. Muders
(MPIfR: Bonn, Germany)

Bonn, September 9, 2010

1 Introduction

Even after decades of active research, the physical origin of the extreme luminosity in distant radio galaxies and quasar still remains speculative. The high luminosity in almost all parts of the electromagnetic spectrum, the rapid and often correlated broad-band variability (radio to VHE), and the ejection of highly relativistic plasma jets are generally explained via the presence of a super-massive black hole (SMBH) located at the center of these so called Active Galactic Nuclei (AGN) (e.g. Rees et al. 1982; Begelman et al. 1984). One assumes that the accretion of matter onto the SMBH leads to a conversion of gravitational energy into heat and radiation, allowing to reach luminosities close to the Eddington limit (100 % conversion efficiency). However, the details of this conversion process and the possible significant role of electro-magnetic forces, BH rotation and general relativistic effects in the region of strong gravitational forces, are still largely unexplained. It is still a big mystery, how powerful radio jets are launched, collimated and accelerated, and which role in detail the black hole, its spin, the surrounding electromagnetic fields and the matter in the accretion disk play (e.g. Narayan 2005).

This is the point, where the technique of Very Long Baseline Interferometry (VLBI) becomes important, playing its role as the perhaps most powerful astronomical imaging method, at least in terms of angular resolution. The angular resolution of an interferometer increases towards shorter wavelength and with the separation of the individual elements of the interferometer (radio telescopes). In the atmospheric window of the radio bands, which basically covers wavelengths in the range from meters to sub-millimeters, the highest angular resolution obviously can be achieved at the short millimeter and sub-millimeter wavelengths. VLBI performed at these shortest, technically just reachable wavelengths, will give the highest angular resolution and will offer the most powerful observing method to study and image directly – with micro-arcsecond scale resolution – the very central regions in galaxies, quasars and other types of AGN (e.g. Krichbaum 1996; Krichbaum et al. 2006a). The very short observing wavelength (high observing frequency) leads to a second, astro-physically relevant advantage: compact galactic and extragalactic radio sources are self-absorbed and optically thick at long radio wavelengths. However, they become optically thin (transparent) towards shorter wavelengths, which facilitates mm- and sub-mm VLBI to observe and image small regions, which are not visible at longer wavelengths. This makes mm- and sub-mm VLBI unique in the sense that it can reach central regions unobservable at longer wavelengths, a big advantage if one aims at the direct imaging of the 'hidden' central engine (the SMBH and the surrounding accretion disk) in an AGN.

Similar to the well established VLBI observations at the longer centimeter wavelengths, global sub-mm VLBI involves telescopes at different continents with separations from each other of a few hundred up to ~ 10.000 km. This leads to an angular resolution of 17 micro-arcseconds at 1.3 mm (230 GHz) and 11 micro-arcseconds at 0.87mm (345 GHz). Translated into units of gravitational (or Schwarzschild) radii, it will be possible for the very nearby objects like the Galactic Center (Sgr A*) and M 87, to reach the scale of the event horizon of the SMBH and the inner region of the accretion disk (last stable orbit) (e.g. Falcke et al. 2000; Broderick & Loeb 2009). When performed with a sufficiently large number of antennas ($N > 5$) and with sufficiently large collecting area and sensitivity, global sub-mm VLBI offers the unique possibility to

directly image and study super-massive black holes and the emission around it (event horizon, ergo-sphere). At 0.87mm wavelength and for the nearest SMBH in the center of our Galaxy (Sgr A*), global sub-mm VLBI with as many as possible participating telescopes in Europe (IRAM), North America (SMA, CARMA, HHT) and in Chile (APEX, ASTE, ALMA) offers an observing beam of almost exactly 1 Schwarzschild radius. This makes Sgr A* (and M87) the prime targets for a previously not possible in depth study of a super-massive black hole and the (likely time-variable) post-Newtonian emission region surrounding it.

2 Previous Work and Present Status

In contrast to global VLBI at 3 mm, which nowadays is performed regularly with the GMVA, VLBI observations at shorter wavelength are still in a phase of technical development and are limited presently by the small number of mm-VLBI capable telescopes, which only recently has started to increase (see Table 1). Single baseline 1 mm-VLBI test experiments performed in the early 90ies, first yielded only marginal, and later – when both IRAM antennas became available – much stronger detections (Padin et al. 1990; Greve et al. 1995; Krichbaum et al. 1997). The combination of the 30 m IRAM telescope on Pico Veleta with a single antenna of the PdB interferometer, which at that time could not yet be phased for VLBI, led to detections of about a dozen of bright AGN with $SNR \leq 35$ and also to the first detection of the Galactic Center radio source Sgr A* with VLBI at 215 GHz (Krichbaum et al. 1998). The latter observation resulted in an upper limit to its size of only $\leq 10 - 15 R_s$.

On the way towards shorter wavelength and trying to establish now also transatlantic source detections, global VLBI pilot experiments were performed first at 2 mm (129 & 149 GHz) (Greve et al. 2002; Krichbaum et al. 2002; Doeleman et al. 2002). These experiments led to source detections first on the Pico Veleta to Metsähovi baseline, and one year later also to detections between Pico Veleta and the 10 m Heinrich Hertz sub-millimeter telescope (HHT) in Arizona.

After having established the technical feasibility of VLBI at the HHT, the next step was to observe at 1.3 mm (230 GHz) and establish transatlantic fringe detections between IRAM and USA also at this shorter wavelength. These observations were performed in April 2003 (Krichbaum et al. 2004b; Doeleman et al. 2005) with the following stations: PV, PdB (now phased), HHT, and Kitt Peak (KP). Problems with the phase stability of the local oscillators at KP and PdB, a relatively high receiver noise at HHT ($T_{sys} \sim 550$ K DSB), and a technical problem with the new MK5 recording system (recording at 512 MBit/s instead of the anticipated 1 Gbit/s), limited the success of this experiment. Despite these problems, still two sources (QSO 3C454.3, BL 0716+714) could be detected on the transatlantic baseline between PV and HHT ($SNR \simeq 7$), marking a new world record in fringe spacing ($\sim 6 G\lambda$) and angular resolution ($30 - 35 \mu\text{as}$ beam). The fact that 50% of the observed sources (18) were also clearly detected on the 0.9 $G\lambda$ long baseline between PV and PdB (at $SNR = 8 - 25$), outlines the high sensitivity of this baseline and marks its importance for future global mm-/sub-mm VLBI.

It took more than 10 years and until very recently, when new VLBI observations at 1.3 mm wavelength were made. In this observation two new VLBI-telescopes (JCMT+SMA and a single CARMA antenna) were made available and combined with the HHT (Arizona). Mainly due to much improved sensitivity (gain by a factor of 3, owing to digital recording and larger bandwidth) and longer VLBI baselines (~ 4000 km from Arizona to Hawaii), a new and smaller size for the Galactic Center radio source could be determined (Doeleman et al. 2008). These observations (and the detection of some other AGN) demonstrate the technical feasibility of VLBI at short mm-wavelengths ($\lambda \leq 1.3$ mm, $\nu \geq 230$ GHz) and open the possibility to study and directly image black holes with mm- sub-mm VLBI.

3 The Project

The main limitations of the previous 2 & 1.3 mm VLBI observations – in addition to the general lack of suitable telescopes – were too high receiver noise, residual phase instabilities in the local oscillator chains of some telescopes. State of the art low noise and single side-band receivers now available at PV, PdB and HHT and an improved phasing stability of PdB (new H-maser, new synthesizer), the time is ripe for the next step towards *building up a globally operating mm-/sub-mm VLBI array*. The main scientific driver is the wish to image with $\sim 10 - 20$ micro-arcsecond scale resolution the central black hole in Sgr A* and in some other nearby AGN (Event Horizon Telescope). With new sub-mm telescopes like the SMA, APEX, the planned LMT and in particular with ALMA, a sufficiently large number of antennas will become operational soon. So it is the right time to think about the construction of a globally operating mm-/sub-mm VLBI array, which provides mikro-arcsecond scale resolution and has good imaging capabilities (high sensitivity, good uv-coverage). In Tables 1 and 2 we give a list of telescopes which are potential partners for building up such an array at 1.3 mm (230 GHz) and in Table 5 at 0.87 mm (345 GHz). The label 'V' in Table 1 indicates, whether a station has already participated in earlier VLBI pilot studies at short millimeter wavelengths (see Krichbaum et al. 2008).

The transition from the analog to the digital VLBI data acquisition system, now offers 1 GHz recording bandwidth (4 GHz are planned) and correspondingly (4-8 times) higher VLBI detection sensitivities. In Table 3, 4, and 6 we summarize achievable baseline sensitivities using the usual and conservative approach of a 7σ single baseline detection threshold. All numbers are calculated for a observing bandwidth of 1 GHz (4 Gbit/s recording rate) and may improve as one will be able to move to larger bandwidths during the next 3-5 yrs.

The recent demonstration of the technical feasibility of 1 mm-VLBI on the long Arizona (HHT) - Hawaii (SMA, JCMT) baseline (4000 km) and the new size limit of only $\sim 4 R_s$ for the Galactic Center Sgr A* obtained by Doeleman et al. (2008) motivate us to propose an active participation of European observatories in global VLBI at 1.3 mm and shorter wavelengths (≤ 0.87 mm).

3.1 mm-VLBI with APEX

In this context we propose to equip the APEX telescope for VLBI experiments at wavelength of 1.3 mm and shorter (provision of H-maser, digital backend, Mark5 disk recorder) and support other stations (IRAM, HHT) in upgrading their existing VLBI equipment (digital backends for wider bandwidth). With regard to its location in the southern hemisphere, the outfit of APEX for mm-/sub-mm VLBI is of crucial importance for the direct imaging of the super-massive Black Hole in the Galactic Center Sgr A* and for immediate tests of Einsteins theory of General Relativity (for details see paragraphs below). As a sub-mm VLBI station, the APEX telescope also can significantly contribute to the micro-arcsecond scale imaging of at least a dozen of other nearby radio-galaxies, such as M 87 (Virgo A), Cen A, Arp 220, NGC 1275 and 3C 120. The location of APEX in the southern hemisphere, makes this station particular important in several aspects:

(i) it provides very long baseline length to both Europe and USA and by this increases the angular resolution of the continental sub-arrays by a large factor (ii) in terms of mutual visibility it connects the European and US subarrays for basically all compact radio sources with declinations $\delta \leq 20^\circ$ and in particular for the Galactic Center, for which APEX will allow to measure closure-phases from Chile to France and Spain, as well as from Chile to Hawaii, California and Arizona (see Fig. 1). (iii) APEX can act as precursor (or pathfinder) for future VLBI with ALMA and can help to strengthen the role of European astronomers in high angular resolution interferometry at sub-mm wavelengths over the next decade.

3.1.1 The role of APEX/ALMA for mm-VLBI in Europe:

In Europe only two major mm-telescopes exist, the IRAM 30 m telescope in Spain (Pico Veleta) and the 6 x 15 m IRAM interferometer in the French Alpes (Plateau de Bure). Although these two antennas perform

excellent and have superior sensitivities, their relative distance of only 1150 km limits the achievable VLBI angular resolution. On the other side of the Atlantic, however, a 4000 km baseline is available, when combining the HHT in Arizona with the antennas in Hawaii. Adding a station in South America (APEX, later ALMA) immediately leads to a 8600 km baseline to PV, respectively a 9400 km baseline to PdB. Furthermore, and very important in view of the detection of expected deviations from point-symmetry in Sgr A*, APEX/ALMA and the IRAM telescopes form a very sensitive closure triangle, eventually facilitating the detection of a predicted 20 min beating in the closure phases, due to Keplerian motion in the last stable orbit (Doeleman et al. 2009).

In this context it is very important to make available the APEX antenna for mm- and sub-mm VLBI as soon as possible. With this antenna the role of the MPIfR (and its partners) in the context of the further development of mm-VLBI towards shorter wavelength would be considerably strengthened, and would allow the European scientists to act as equal partner with US-American colleagues, who begun to build up are a North-American sub-mm VLBI network. The experience gathered during the VLBI-installation of APEX and the equipment brought to APEX (e.g. hydrogen maser, recording terminals, pressure housings) will also be important for the later use of ALMA in VLBI. In this context, APEX can be used as a pathfinder for VLBI with ALMA.

The direct access to a mm-/sub-mm VLBI antenna, which not only can operate at 1.3 mm, but also should deliver good results at shorter wavelength (at 0.8 mm, 345 GHz), furthermore will allow the partners of the APEX consortium to gather experience with the new technology of wide-band VLBI recording, which is now being developed, and will put them in an excellent strategical position, when it comes to first VLBI experiments in the so far still unexplored VLBI wavelength range at and below 0.87 mm (> 345 GHz). Also in this context, the installation of VLBI equipment (H-maser, digital backend, Mark5 disk recorder) for APEX will be very important and demands immediate action.

3.1.2 The final aim: mm-VLBI with ALMA

From Tables 3, 4, & 6 the dramatic gain in sensitivity, when adding ALMA is obvious. The resulting better detection and imaging sensitivities will allow to study many more sources than today is possible. In terms of sensitivity, the addition of ALMA will put mm-VLBI in a situation comparable to what is possible today with VLBI at cm-wavelength. The participation of ALMA in future mm-VLBI will not only boost the sensitivity of global mm-VLBI, but also will facilitate future VLBI experiments at even shorter wavelength, than it is possible now (1.3 mm). In particular for partially resolved sources (like Sgr A* and probably many other AGN), a high sensitivity on the 'other' end of a long VLBI baseline will be crucial for any fringe-detection and for achievement of the highest possible angular resolution.

Before ALMA becomes available for mm-VLBI, a number of technical problems have to be solved. The most important one will be to develop and establish the phasing of ALMA for its use as a tight array in VLBI-mode. At present the development of a VLB-array phasing processor isn't planned, nor are technical details about signal digitization and phase-stable down-conversion, etc. properly elaborated. The development and installation of VLB-array phasing for an instrument like ALMA is a complicated task, and probably requires the formation of an international working-group of technically skilled partners. Realistically, we may expect the operation of ALMA as a phased array in VLBI mode only several years after its official commissioning as a fully functional local interferometer, i.e. not before ~ 2015 .

In order to provide a high image quality, a good filling of the uv-plane is very important (earth-rotation aperture synthesis). The combination of APEX with one or several single ALMA antennas at a time, when ALMA is not yet fully available for phased array VLBI operation, will be extremely useful for a number of reasons. It will provide the necessary short uv-spacings, often lacking in VLBI experiments. The short uv-spacings are not only of great importance for the calibration of the whole mm-VLB array and for the determination of the total source flux, but also – when polarisation will be measured – for the determination of the absolute (total) polarisation angle. From mm-VLBI at 3 mm wavelength it is known, that a substantial fraction of the VLBI flux is not concentrated in the VLBI core region, but could be distributed along the

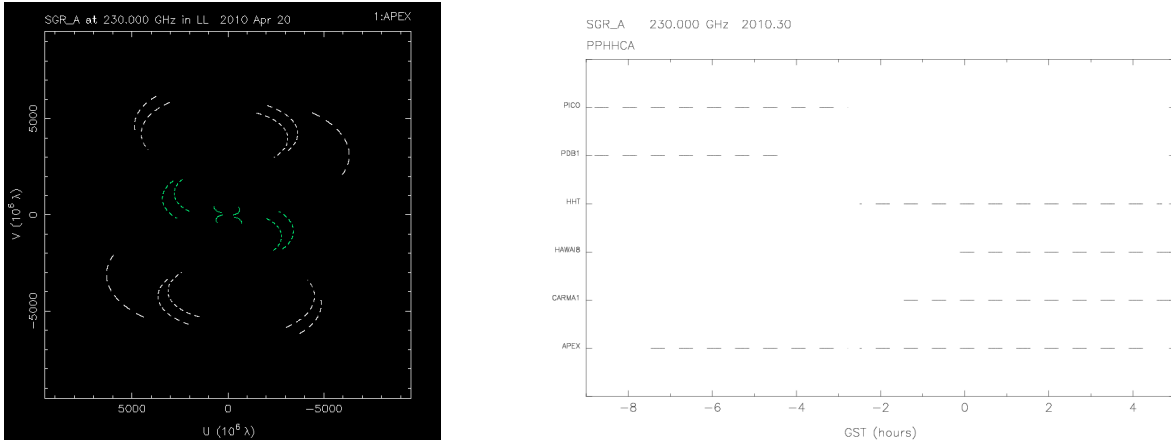


Figure 1: Left: Plot of the uv-coverage for a 1.3mm VLBI experiment on Sgr A* with the following stations: Pico Veleta, Plateau de Bure, Heinrich-Hertz Telescope, Hawaii, CARMA, and Apex. Right: Mutual time of common source visibility between the stations.

larger milli-arcsecond scales (e.g. along a jet, or for stellar SiO-masers along a ring). The imaging of such extended structures requires a large field of view, which is provided by sufficiently short ALMA-to-APEX and inter-ALMA baselines (km's). The possible combination of APEX with the Japanese ASTE telescope (located a few kilometers from APEX) will be of similar value.

4 Scientific Motivation

In the paragraphs below we briefly address the main scientific motivation for studies of compact galactic and extragalactic radio sources and our proposal to equip APEX for mm- and sub-mm VLBI. Our main motivation is governed by the wish to image the centers of galaxies, quasars and other AGN with such a high angular and spatial resolution, so that we can directly image the innermost region of the radio source, i.e. the BH, the disk surrounding it and the emanating jet, and by this test the paradigm of the so called 'central engine'. This 'central engine' drives most of the observed AGN activity (spectral energy distribution, variability, etc.) and is presumably a Black Hole surrounded by an accretion disk, some magnetic fields, and a one or two-sided outflow (wind, jet) emanating either from the accretion disk or the Black Hole itself. This triggers our second main motivation, in which we would like to understand how the Black Hole/accretion disk systems is coupled to the observed powerful radio jets, addressing the very fundamental question of how the powerful radio jets are generated and launched.

4.1 SgrA*

There is now overwhelming evidence for the existence of a super massive black hole of $\sim 4 \cdot 10^6 M_{\odot}$ at the center of our Galaxy (Gillessen et al. 2009; Ghez et al. 2008). Millimeter wavelength VLBI allows us to see through the interstellar scattering screen that broadens the radio images of Sgr A* at longer wavelengths with a λ^2 dependence. Over the last decade VLBI observations in the cm- and mm-bands have set important size limits on the emission region (Rogers et al. 1994; Krichbaum et al. 1998; Doeleman et al. 2001; Shen et al. 2005; Bower et al. 2006) and so far show no deviation from an east-west elongated point source.

New 1.3 mm VLBI observations performed in April 2007 using a three station VLBI array (HHT, JCMT, CARMA(1)) and recording for the first time at a higher recording rate(4 Gbit/s), now reveal – with the assumption of a spherical Gaussian brightness distribution – a new size limit of $\sim 3.7 R_s$ ($1 R_s = 10 \mu\text{as}$

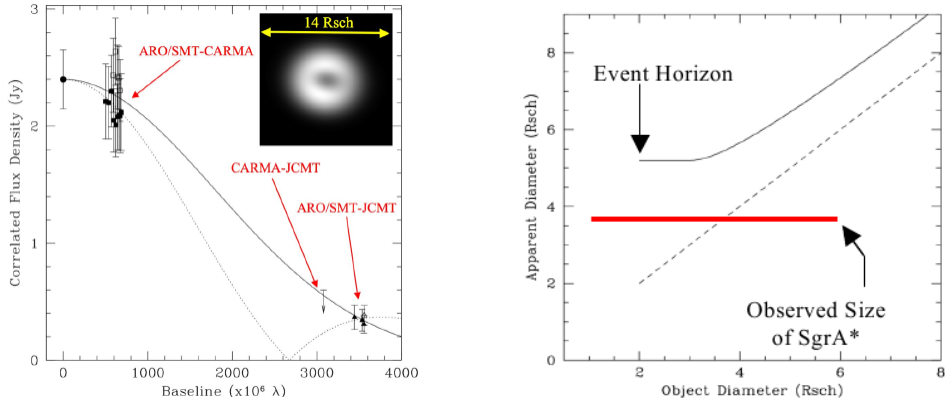


Figure 2: Left: Correlated flux versus projected baseline length for Sgr A* for the 1.3 mm VLBI observation of April 2007 (Doeleman et al. 2008). The solid line marks a Gaussian profile of $37 \mu\text{as}$ size. The dotted curve shows a profile for a shadow model (shown as insert), with $35 \mu\text{as}$ inner diameter and $80 \mu\text{as}$ outer diameter. Replacing JCMT by the eSMA (phased SMA + JCMT + CSO) and increasing the sensitivity of CARMA should allow to detect the source on all baselines. Currently only an upper limited for the correlated flux is obtained on the CARMA-JCMT baseline, not allowing to distinguish between the models. Right: A symmetric emitting surface surrounding a black hole is gravitationally lensed and appears larger than its true diameter. Here, the apparent size is plotted as a function of actual object size: the solid line shows the apparent diameter with lensing, the dashed line without lensing (no rotation of BH). The observed intrinsic size at 1.3 mm is smaller than the expected size, possibly indicating that we see a compact emission region, which is either a fraction of the accretion disk, or a crescent like structure, distorted by relativistic aberration. Image courtesy: S. Doeleman et al.

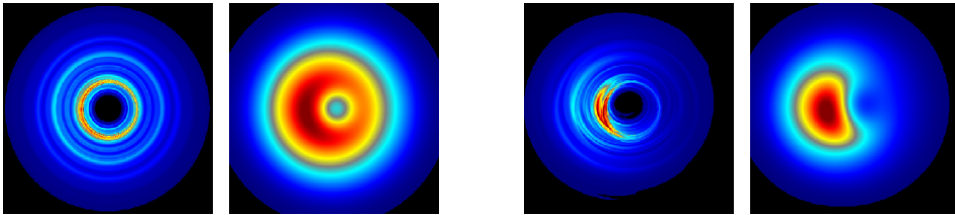


Figure 3: Image of the accretion disk viewed at a wavelength of 1mm and seen at an inclination of 5° (left) and 30° (right). Each frame on the left is from a simulation with ‘infinite’ resolution, while on the right the map has been convolved with a circular Gaussian beam corresponding to a 8000 km VLBI baseline. Images taken from Noble et al. (2007).

$= 0.1 \text{ AU}$), which is significantly smaller than the expected size of $5 - 6 R_s$ for relativistically aberrated emission near the event horizon (Doeleman et al. 2008) (see Fig. 2, right). The detection of Sgr A* on the short HHT-CARMA and the long HHT-JCMT baseline and the lack of the detection on the intermediate JCMT-CARMA baseline opens the possibility for a non-gaussian, crescent or toroidally shaped brightness distribution (see Fig. 2, left). Alternatively it may be possible that one has seen a compact sub-region in the accretion disk, which would favor the hot-spot model, e.g. Broderick & Loeb 2006b; Eckart et al. 2008).

In Figure 3 we show simulated images of the accretion disk, which show an asymmetric brightness distribution caused by the relativistically enhanced emission region on the approaching side of the disk (Noble et al. 2007). The exact shape of the brightness distribution mainly depends on the mass of the black hole (which determines the orbital period and the Doppler-enhancement), the spin of the Black Hole, and

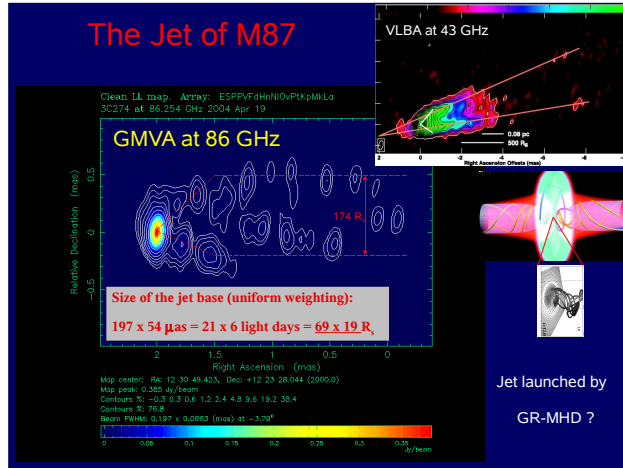


Figure 4: VLBA observations at 43 GHz (top left, Walker et al. 2008a) and GMVA observations at 86 GHz (large figure, Krichbaum et al. 2008) reveal a conically opening VLBI jet. The 86 GHz image sets a new stringent limit to the size of the jet base (nozzle) of less than $15 R_s$. Future VLBI at 1.3 mm and 0.8 mm will give a 3 – 4 times higher resolution, allowing to see how the jet is generated.

the inclination of the disk relative to the observer. A detailed comparison of such simulations with future VLBI images obtained at 1.3 mm and shorter wavelengths will allow to put hard constraints on these very fundamental parameters (Broderick & Loeb 2006a; Broderick et al. 2009; Fish et al. 2009). It is clear that new observations with better uv-coverage and higher sensitivity are needed to discriminate between the models and to be able to actually produced a reliable 1.3 mm VLBI map of the emitting region.

In Figure 1 we show the uv-coverage for a future VLBI experiment with the following stations: Pico Veleta, Plateau de Bure, Heinrich-Hertz Telescope, Hawaii (eSMA), CARMA, and APEX. The white lines outline the uv-tracks from the addition of APEX, which not only more than doubles the angular resolution, but also leads to a more circular observing beam (when compared to observations without a station in the southern hemisphere). On the right of Figure 1 the time of common source visibility is shown for the 6 stations. From this it is very clear that the participation of a station in Chile is essential, as it connects the very sensitive European telescopes (PV, PdB) with the smaller and therefore less sensitive stations in the US (SMA, HHT, CARMA).

4.2 M87

The giant elliptical galaxy M87 (Virgo A, NGC 4486, 3C 274) is one of the closest radio galaxies with a prominent radio jet ($z=0.00436$, $D=16.75$ Mpc). Like Sgr A* it is underluminous by many orders of magnitude in comparison to the Eddington limit. M87 is located on the northern sky and for the presently existing mm-VLBI stations it is more easy to observe than Sgr A* (higher elevation at the telescopes, more circular observing beam, better uv-coverage). Furthermore, M87 is not affected by interstellar scattering and image broadening, which has lead to complications in the interpretation of the structure of Sgr A*. Since M87 has a prominent radio-jet, this source probably is – at least with regard to jet physics – more representative for the large population of other AGN (radio galaxies, blazars) than Sgr A*.

With a central BH mass of $3 \cdot 10^9 M_\odot$, 800 times more massive than Sgr A*, and a 2000 times larger distance, the spatial resolution in a global mm-VLBI image in M87 is only a factor of 2.5 worse than for Sgr A* ($1 R_s = 3.6 \mu\text{as}$ for M87, $1 R_s = 10 \mu\text{as}$ for Sgr A*). At 1.3 mm wavelength and with a typical observing beam of $\sim 17 \mu\text{as}$ it is therefore possible to reach a scale of $4.7 R_s$, which is of order of the size of

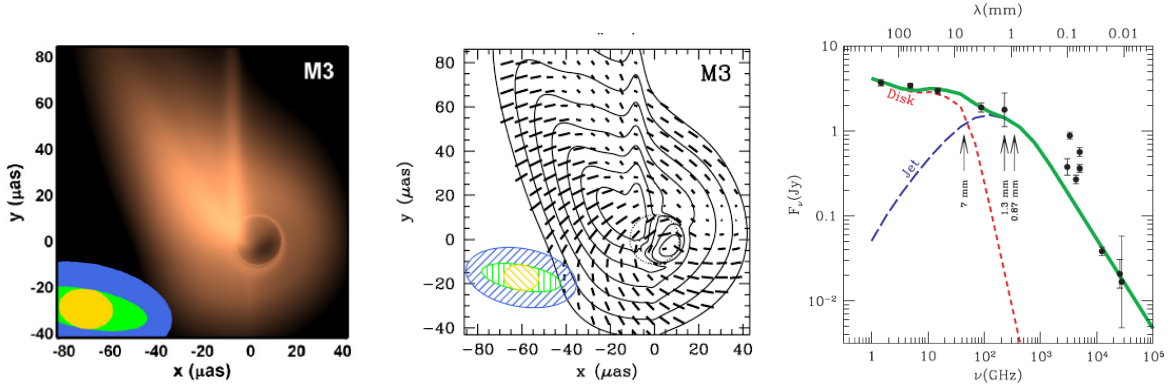


Figure 5: Simulated images of the Black Hole silhouette and inner jet in M87. On the left a total intensity map at 1.3mm is shown, and next to it on the right the linear polarization vectors. The ellipses in the lower left provide an estimate of the beam size for arrays consisting of US-telescopes only (blue), adding European telescopes and the LMT (green), and adding APEX (yellow). The plot on the right shows the radio-to-submm spectrum of M87, with jet and disk indicated by lines. Plots adopted from Broderick & Loeb (2009).

the relativistically aberrated silhouette of the event horizon. The higher mass of M87 implies a dynamical timescale of ~ 5 hrs and an orbital timescale of 2 – 18 days (depending on BH spin). Thus M87’s structure remains stable during the time of a VLBI observation (5-15 hrs), in contrast to Sgr A*, which can vary on timescales of ~ 15 min to a few hours. The stationarity of M87 during a VLBI observations allows to achieve a higher dynamic range in the images and even gives the opportunity to make sequences of images over many days (movie). M87 therefore is the ideal object for highest angular resolution VLBI studies, which address the question how a powerful and relativistic jet couples to the BH/accretion disk system and how its structure evolves.

VLBI images at 43 & 86 GHz (Fig. 4) show an edge-brightened conically opening jet originating from a core of less than $15 R_s$ in size at 86 GHz (see Fig. 4, Ly et al. 2007; Krichbaum et al. 2004b; Walker et al. 2008b; Krichbaum et al. 2008). The relatively large opening angle and the hollow jet structure point towards a MHD jet, which is launched either via the magnetic sling-shot process (Blandford & Payne 1982; Camenzind 1990) with magnetic field lines anchored in the rotating accretion disk (BP-process), or via a direct extraction of rotational energy from a Kerr Black Hole (BZ-process) (Blandford & Znajek 1977). The observed small size of the jet footpoint (VLBI core) and the large opening angle ($\theta \sim 40 - 60^\circ$) pose some difficulties for the BP-process, which is based on widely open field lines to obtain a long leverarm for the plasma acceleration (B field anchored in the rotating accretion disk). In this model the light cylinder has a radius of at least $10 - 50 R_s$ (Camenzind 1990; Appl & Camenzind 1992; Fendt & Memola 2001), which sets a lower limit to the jet width of $\geq \gamma \cdot 2R_L$ (Tomimatsu & Takahashi 2003). With a typical jet Lorentz-factor of $3 \leq \gamma \leq 6$ (Dodson et al. 2006; Kovalev et al. 2007; Walker et al. 2008b), one would therefore expect a jet width of $\geq 60 - 600 R_s$, which is larger than the limit of $< 15 \times 56 R_s$ obtained from 3 mm-VLBI (Krichbaum et al. 2006b, 2008). Progress in the theoretical understanding and modeling of rotating (Kerr) BH’s and magnetized disks/jet systems now point towards a jet launching process, which is directly coupled to the spin of the BH (Meier et al. 2001; Koide et al. 2002). In fact, a faster rotating black hole allows more energy to be extracted and predicts a conical/hollow jet (Hawley & Krolik 2006; Keppens et al. 2008), which is actually fast enough ($\gamma \leq 10$) and even stable against the disruptive kink- (or screw) MHD-instabilities (Tomimatsu et al. 2001; McKinney & Blandford 2009). The lightcylinder radius for spinning BH’s is smaller than for the non-rotating BH’s, since the helical and collimating magnetic field

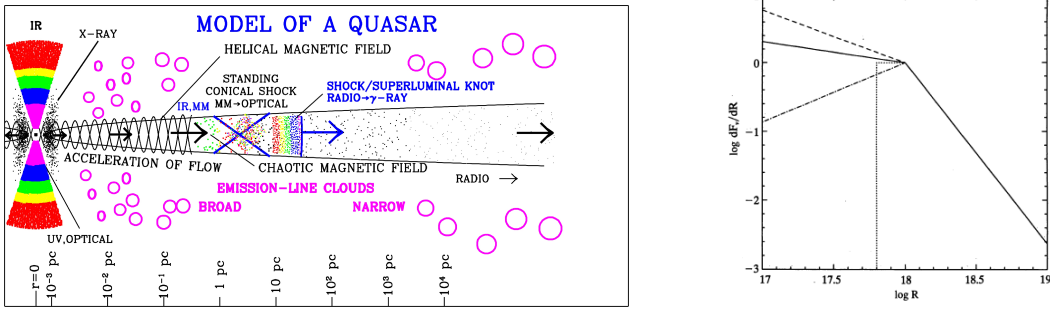


Figure 6: Right: A schematic view of an AGN jet. The acceleration and collimation of the jet happens on sub-parsec scales. Left: Depending on the details of the acceleration process and the jet composition, the brightness temperature of the inner jet will decrease or increase with distance from BH. mm-VLBI can provide the spatial resolution to image these regions and distinguish between fundamentally different classes of jet models. Figures taken from Marscher (1995, 2006).

lines are generated much closer to the spin axis of the BH than in the BP-models. It is therefore tempting to interpret the observed jet structure in M 87 as evidence in favor of the BZ-process and a significant BH-spin. An important consequence of this is that one perhaps can use the measured jet-width to constrain the spin of a BH.

Future VLBI imaging with an angular resolution high enough to see the ‘connection’ between disk, BH, and jet base will therefore help to substantially improve our knowledge about the details of the process of jet generation. VLBI at 1.3mm and shorter wavelengths will provide the angular and spatial resolution needed for this. We like to point out that the exact shape of the jet at its footpoint, its size, width and brightness as function of distance from the BH are very important parameters for the detailed modeling of such systems. In Figure 5 we show as an example a simulated VLBI map of M 87 resulting from fully relativistic GRMHD simulations around an accreting and rotating SMBH (McKinney & Blandford 2009). Horizon-resolving VLBI images are very important as they allow to distinguish between the many different models and simulations about jet formation. Each of these simulations uses different ad-hoc assumptions and often quite different sets of parameters, some of them perhaps not well matched to reality. A detailed mm-VLBI imaging combined with the comparison of the models, will help to better constrain the parameter space and by this will lead to more realistic assumptions about geometry and physical conditions near SMBH’s.

4.3 A 1mm AGN VLBI Survey and the acceleration of AGN jets

VLBI-surveys at centimeter wavelengths (3.6 cm CJF, 2 cm MOJAVE) reveal the existence of jets in hundreds of AGN and a wide variety of structures in them (Kellermann et al. 2004; Britzen et al. 2008). These surveys mainly address source morphologies, kinematical aspects in jets and the statistical distribution of these properties among the different source classes (e.g. quasars, BL Lacs, radio-galaxies) and can be used to test unified scheme models of AGN (e.g. Barthel 1989; Antonucci 1993; Urry & Padovani 1995). Surveys at higher frequencies in general can penetrate deeper into the AGN and are of high interest in view of the exact details of the physical properties of the – at longer wavelengths unresolved – cores, the details of the jet launching process and the statistical properties of the source samples in still unexplored frequency ranges (e.g. Marscher 1995, 2006).

An AGN jet consist of a region where it is launched and collimated (inner jet, sub-parsec scales) and an outer region, where it propagates (see Fig. 6). Near the core jets are often strongly curved, indicative of spatially curved magnetic fields (helix) and/or jet precession. The high angular resolution imaging with

mm- and sub-mm VLBI will trace the jets closer to their origin and will provide information about the physical origin of the often observed jet curvature and acceleration.

As pointed out by Marscher (1995), the internal particle composition of a radio jet is still unknown (hadronic, leptonic) and the role of the magnetic field in the jet acceleration is unclear. One way to discriminate between very different classes of jet-models is the measurement of the brightness temperature of the jet. Depending on the details of the acceleration process and the jet composition, the brightness temperature of the inner jet will decrease or increase with distance from BH. Following this approach, attempts have been made to measure the brightness temperature in combining available data from cm-VLBI and adding new data obtained from the GMVA at 86 GHz (Lobanov et al. 2000; Lee et al. 2008; Krichbaum et al. 2008). These results confirm the existence of – at this frequency – still unresolved core components, but also indicate the possibility of the jet brightness temperature decreasing towards the core and on sub-pc scales. This could mean that most of the jet acceleration takes place in a small region of much less than one parsec. VLBI observations at higher frequencies should show this effect more clearly and will shed light on the question, if all AGN-jets behave like this and if there are differences in the brightness temperature gradients between the different AGN types and their intrinsic luminosities.

The EGRET and FERMI satellite mission reveal hundreds of AGN being bright at gamma-rays and strongly variable. It is assumed that the gamma-rays are produced by the inverse Compton process (SSC, EC) either in the jet or near the nucleus in the matter surrounding it (accretion disk, BLR). An important parameter for the modeling of the gamma-ray production is the degree of compactness of the core and jet, its morphology and kinematics on scales of less than 1000 Schwarzschild radii, the region commonly assumed to be the place of the gamma-ray production. It is therefore important to observe gamma-bright compact radio sources at the shortest possible wavelength and with the highest achievable angular resolution.

It will be therefore very important to image a sample of mm-bright AGN with the aim to study their compactness at the highest possible frequency and with the highest achievable angular resolution. In previous 1 mm- and 2 mm VLBI pilot experiments it has already been demonstrated that the compactness of the VLBI cores is high, allowing to detect them even on the longest transatlantic baselines (Krichbaum et al. 2004a,b, 2006a). A VLBI detection survey of the $\sim 50 - 100$ brightest AGN will offer a good opportunity to measure core and jet sizes and statistically related them to source classification, luminosity in radio, optical and gamma-ray bands, and the known jet speed. We note that there are about 15 – 20 nearby radio galaxies (distance $D \leq 200$ Mpc), which are probably bright enough to be observed with the existing mm-telescopes (Table 2). For these objects a more detailed imaging is very interesting, as it would allow to make maps with a spatial resolution of only $\leq 100 R_s$ and by this probe the jet production region in a larger sample of objects than just for Sgr A* and M 87.

The observation of mm-bright radio-galaxies and quasars at larger cosmological distances ($z > 2$) allow to image BH-jet systems at an earlier stage of their cosmological evolution. Since in the source rest-frame the frequency is blue-shifted by a factor of $(1 + z)$, such observations would probe the central regions at even higher rest-frame frequencies, opening the fascinating possibility to look in synchrotron-self absorbed sources through the final opacity surface, beyond which the source must become optically thin. The study of the compactness of sources as function of their redshift (distance) is therefore an important tool to determine the synchrotron turnover frequency and magnetic field strength in the most compact component of an AGN.

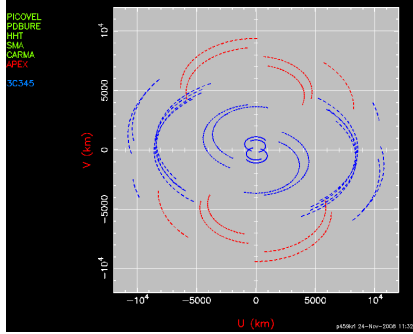
In view of planned space VLBI missions (VSOP-2, RADIOASTRON) the knowledge about the degree of compactness of the future space-VLBI targets is important. Observing these sources at the highest possible frequencies with VLBI will ensure their detectability also at the longer wavelengths planned for VSOP2 (8, 22, 43 GHz) (Hirabayashi et al. 2004; Tsuboi 2008).

In Figure 7 we plot the uv-coverage of a simulated VLBI experiment for sources with northern declination. The contribution of APEX to such an experiment is still remarkable as it can observe sources with declinations of up to $\delta \leq 52^\circ$.

APEX: Mutual Visibility for Northern Sources

geographical latitude of APEX: $\phi = -23^\circ$
 culmination height above horizon: $elv = 67^\circ - \delta$
 \Rightarrow northern declination limit $\delta \leq (67^\circ - \text{horizon } (15^\circ)) \approx +52^\circ$

3C345, $\delta = 39.8^\circ$ (6 hrs with APEX)



3C454.3, $\delta = 16.1^\circ$ (8.5 hrs with APEX)

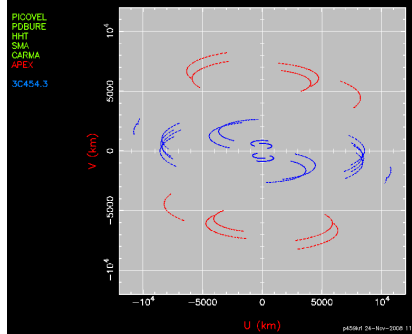


Figure 7: Plot of the uv-coverage for two northern hemisphere sources with APEX: 3C345 at declination $+39.8^\circ$ (left) and 3C454.3 at declination $+16.1^\circ$. For both cases, APEX adds important data points to the uv-plane (red lines). With a local horizon at about $elv \geq 15^\circ$, APEX is able to observe sources with declinations of $\delta \leq 52^\circ$.

5 Pilot Studies at $870 \mu\text{m}$

The scientific motivation for VLBI observations at 0.87 mm (345 GHz) is the same as for 1.3 mm (230 GHz). Observations at this shorter wavelength are the next logical step and are motivated by the higher angular resolution and the chance to image the silhouette around BHs with even higher accuracy. VLBI observations at the shorter wavelength of 0.87 mm will be more challenging than observations at 1.3 mm , due to the lower sensitivity of the array and the reduced number of available stations (Table 5). Again, the participation of ALMA will greatly improve the sensitivities. VLBI observations at 0.87 mm are scientifically interesting, as they provide a smaller observing beam at a higher frequency, where absorption effects are less pronounced. With the advent of more mm-telescopes during the next years, ongoing receiver development and the attempts to further increase the VLBI observing bandwidth up to at least 4 GHz (32 Gbit/s using 2 polarizations), it should be possible to find fringes on the brightest AGN and Sgr A*. Using the same arguments as outlined before, it is therefore envisaged to perform pilot studies and detection tests during the next 2-5 years, with the aim to establish regular sub-mm VLBI observations in the near future.

6 Synergies

Observational results from mm- and sub-mm VLBI will be scientifically interesting by its own, but also must be seen in a broader context. Successful and modern AGN research is broad-band in energy and covers all spatial scales. In AGN-jets, mm-/sub-mm VLBI probes the spatial scales where gamma-rays are produced, and by this produces a large overlap with the communities which study AGN at the highest energies (FERMI, HESS, MAGIC). With regard to the flux density variability, the detection of newly ejected

jet-plasma in its earliest evolutionary stages is facilitated by mm-/sub-mm VLBI imaging. The monitoring of such evolving structures will help to better understand jet formation, allowing to test modern GR-MHD jet simulations. For Black Holes and the related effects of General Relativity there is a strong overlap with theorists, which are interested in an experimental/observational tests of their ideas and models, often not checkable locally (on Earth, near the Sun). The combination of the results from mm-/sub-mm VLBI with VLBI images obtained at the longer wavelengths and with space-VLBI (VSOP-2, RADIOASTRON) will lead to an improved understanding of the spectral properties of the studied objects (spectral index maps and polarization maps with matching resolution). High angular resolution studies will be needed as follow up for sources observed/detected with the sub-mm satellite missions (Herschel, Planck), and for sources where local interferometers (CARMA, SMA, ALMA) do not provide sufficient angular resolution.

Being at the technical frontier, VLBI at short wavelengths stimulates progress and new developments in many aspects, like e.g. for a better correction of atmospheric effects in interferometric data (water vapor radiometry, phase correction), an improved phasing of antennas in local interferometers, the development of more sophisticated and new software for correlators and post-correlation data analysis (fringe fitting, calibration, atmospheric phase-correction, imaging software), etc. Due to its challenging nature and the possibility to reach the event horizon in black holes, mm-/sub-mm VLBI has the potential to attract new users and scientifically interested young people. It is also important to train the next generation of students for being experts in mm-interferometry, which is needed when ALMA comes in full operation.

Table 1: Possible antennas for future mm- and sub-mm VLBI

Name	Country	D [m]	Alt. [m]	Surf. [μ m]	150 [GHz]	230 [GHz]	345 [GHz]
Surface < 50 μ m							
SMA ^a	HI, USA	8x6	4100	12	-	+	+
HHT-SMTO	AZ, USA	10	3100	15	V	V	+
APEX	Chile	12	5000	18	?	+	+
ASTE	Chile	10	4860	20	-	?	+
CSO	HI, USA	10	4100	25	?	+	+
JCMT	HI, USA	15	4100	25	?	V	+
Surface 50 – 100 μ m							
Pl.de Bure ^b	France	36.7	2550	55	+	V	+
Pico Veleta	Spain	30	2900	67	V	V	+
CARMA ^c	CA, USA	31.4	2200	30-60	?	V	+
SEST ^d	Chile	15	2300	70	?	?	?
Kitt Peak	AZ, USA	12	2000	75	V	+	-
Metsähovi	Finland	14	Sea L.	100	V	-	-
under construction or planned							
ALMA	Chile	50x12	5000	25	+	+	+
LMT	Mexico	50	4600	70	+	+	+
CCAT	Chile	25	5600	10	-	+	+

Notes:

^a: eSMA: phased array operation of SMA+CSO+JCMT is planned

^b: VLBI phasing with limited bandwidth (≤ 500 MHz)

^c: inhomogeneous array (6x10m+9x6m)

^d: presently mothballed

Col. 1 and col. 2 give telescope and location, col. 3 the antenna diameter, col. 4 the altitude, col. 5 the surface rms. Columns 6-8 summarize the suitability for mm-VLBI for the given observing band, using the following symbols:

"V" : VLBI successfully done, receiver available; "+" : in principle possible, receiver available or planned;

"?" : perhaps possible, but presently no receiver; "-" : not possible

Table 2: Antenna properties at 230 GHz

Antenna	Id	Diameter [m]	Surface [μm]	Eff.	gain [K/Jy]	SEFD [Jy]	comment
Pico Veleta	PV	30	67	0.39	0.101	1485	
Plateau de Bure1	PdB1	15	55	0.45	0.029	5182	single antenna
J.Clerk Maxwell	JCMT	15	25	0.57	0.036	4141	
Submm Array	SMA	17	12	0.59	0.049	3093	phased array: 8x6m
APEX	Ap	12	18	0.58	0.024	6295	
CARMA1	Ca1	10.4	60	0.43	0.013	11373	one 10.4m dish
Heinrich Hertz	HHT	10	15	0.59	0.017	8979	
Plateau de Bure	PdB	36.7	55	0.45	0.174	864	phased array: 6x15m
CARMA	Ca	31.4	60	0.43	0.120	1250	phased array: 6x10.4m + 9x6.1m
Hawai8	eSMA	24.9	25	0.57	0.100	1500	phased SMA+JCMT+CSO
ALMA1	Al1	12	25	0.57	0.023	6469	single antenna
ALMA	Al	84.9	25	0.57	1.159	129	phased array: 50x12m

Note: System equivalent flux densities (SEFD:= $T_{\text{sys}}/\text{Gain}$) are calculated assuming system temperatures of ~ 150 K (SSB) and including the atmosphere. If not known otherwise, the effective aperture efficiency η_A was estimated from the Ruze formulae, which at 230 GHz and in convenient units yields: $\eta_a = 0.7\eta_B \exp -(9.666 \cdot 10^{-3} \mu_{[\text{m}]})^2$, with a typical beam efficiency of $\eta_B = 0.85$.

Table 3: Expected 7σ detection thresholds in [Jy] at 230 GHz
(conservative approach: no array phasing yet at PdB, SMA and Carma in 2010-2011)

	PdB1	JCMT1	CARMA1	HHT	APEX
Pico	0.154	0.138	0.230	0.201	0.169
PdB1	-	0.258	0.429	0.376	0.316
JCMT	-	-	0.385	0.337	0.284
CARMA1	-	-	-	0.561	0.472
HHT	-	-	-	-	0.413

Note: Detection sensitivities are calculated assuming VLBI recording at a rate of 4 Gbit/s (1 GHz bandwidth, 2 bit sampling), coherent integration of $t_{\text{coh}} = 10$ sec, and a 7σ fringe detection threshold. The array sensitivity would be $63 \text{ mJy} / \sqrt{t_{\text{int}}/10\text{sec}}$.

Table 4: Expected 7σ detection thresholds in [Jy] at 230 GHz
(optimistic approach: fully phased arrays at PdB, CARMA, Hawaii, and ALMA)

	PdB	eSMA	CARMA	HHT	APEX	ALMA
Pico	0.063	0.083	0.076	0.201	0.169	0.024
PdB	-	0.063	0.058	0.153	0.129	0.019
eSMA	-	-	0.076	0.202	0.170	0.024
CARMA	-	-	-	0.185	0.155	0.022
HHT	-	-	-	-	0.413	0.059
APEX	-	-	-	-	-	0.050

Note: Detection sensitivities are calculated assuming VLBI recording at a rate of 4 Gbit/s (1 GHz bandwidth, 2 bit sampling), coherent integration of $t_{\text{coh}} = 10$ sec, and a 7σ fringe detection threshold. The array sensitivity would be $25 \text{ mJy}/\sqrt{t_{\text{int}}/10\text{sec}}$ without ALMA, and $9.7 \text{ mJy}/\sqrt{t_{\text{int}}/10\text{sec}}$ with ALMA.

Table 5: Antenna characteristics for a VLBI pilot experiment at 345 GHz

Antenna	Id	Diameter [m]	Surface [μm]	Eff.	gain [K/Jy]	SEFD [Jy]	comment
Pico Veleta	PV	30	67	0.24	0.061	4982	
Plateau de Bure1	PdB1	15	55	0.32	0.020	14684	single antenna
J.Clerk Maxwell	JCMT	15	25	0.53	0.034	8900	
APEX	Ap	12	18	0.56	0.023	13069	
Heinrich Hertz	HHT	10	15	0.57	0.016	18429	
Plateau de Bure	PdB	36.7	55	0.32	0.123	2447	phased array
Hawai8	eSMA	24.9	25	0.53	0.093	3223	phased array

Note: System equivalent flux densities (SEFD:= $T_{\text{sys}}/\text{Gain}$) are calculated assuming system temperatures of ~ 300 K (SSB) and including the atmosphere. The effective aperture efficiency η_A was estimated from the Ruze formulae, which at 345 GHz and in convenient units yields: $\eta_a = 0.7\eta_B \exp -(1.444 \cdot 10^{-2} \mu_{[\text{m}]})^2$, with a typical beam efficiency of $\eta_B = 0.85$.

Table 6: Expected 7σ detection thresholds in [Jy] at 345 GHz
(realistic approach: only two or 3 telescopes in 2011-2015)
(optimistic approach: fully phased arrays: PdB, eSMA, ALMA after 2015)

	PdB1	JCMT	HHT	APEX	PdB	eSMA	ALMA
Pico	0.477	0.366	0.534	0.445	0.193	0.221	0.068
PdB1	-	0.639	0.932	0.777	-	0.387	0.018
JCMT	-	-	0.715	0.596	0.258	0.297	0.090
HHT	-	-	-	0.869	0.376	0.432	0.132
APEX	-	-	-	-	0.314	0.361	0.110
PdB	-	-	-	-	-	0.156	0.048
eSMA	-	-	-	-	-	-	0.055

Note: Detection sensitivities are calculated assuming VLBI recording at a rate of 4 Gbit/s (1 GHz bandwidth, 2 bit sampling), coherent integration of $t_{\text{coh}} = 10$ sec, and a 7σ fringe detection threshold. The array sensitivity would be $177 \text{ mJy}/\sqrt{t_{\text{int}}/10\text{sec}}$ when observing with Pico, PdB1, JCMT, HHT and APEX. If instead of PdB1 and JCMT the phased arrays PdB, eSMA and ALMA are included, the array sensitivity would be $28 \text{ mJy}/\sqrt{t_{\text{int}}/10\text{sec}}$.

References

- Antonucci, R. 1993, *ARA&A*, 31, 473
- Appl, S. & Camenzind, M. 1992, *A&A*, 256, 354
- Barthel, P. D. 1989, *ApJ*, 336, 606
- Begelman, M. C., Blandford, R. D., & Rees, M. J. 1984, *Reviews of Modern Physics*, 56, 255
- Blandford, R. D. & Payne, D. G. 1982, *MNRAS*, 199, 883
- Blandford, R. D. & Znajek, R. L. 1977, *MNRAS*, 179, 433
- Bower, G. C., Goss, W. M., Falcke, H., Backer, D. C., & Lithwick, Y. 2006, *ApJ*, 648, L127
- Britzen, S., Vermeulen, R. C., Campbell, R. M., et al. 2008, *A&A*, 484, 119
- Broderick, A. E., Fish, V. L., Doeleman, S. S., & Loeb, A. 2009, *ApJ*, 697, 45
- Broderick, A. E. & Loeb, A. 2006a, *ApJ*, 636, L109
- . 2006b, *MNRAS*, 367, 905
- . 2009, *ApJ*, 697, 1164
- Camenzind, M. 1990, *Reviews in Modern Astronomy*, 3, 234
- Dodson, R., Edwards, P. G., & Hirabayashi, H. 2006, *PASJ*, 58, 243
- Doeleman, S. S., Fish, V. L., Broderick, A. E., Loeb, A., & Rogers, A. E. E. 2009, *ApJ*, 695, 59
- Doeleman, S. S., Phillips, R. B., Rogers, A. E. E., et al. 2002, in *Proceedings of the 6th EVN Symposium*, ed. E. Ros, R. W. Porcas, A. P. Lobanov, & J. A. Zensus (Bonn, Germany: MPiFR), 223
- Doeleman, S. S., Phillips, R. B., Rogers, A. E. E., et al. 2005, *ASP Conference Proceedings*, 340, 605
- Doeleman, S. S., Shen, Z.-Q., Rogers, A. E. E., et al. 2001, *AJ*, 121, 2610
- Doeleman, S. S., Weintroub, J., Rogers, A. E. E., et al. 2008, *Nature*, 455, 78
- Eckart, A., Schödel, R., García-Marín, M., et al. 2008, *A&A*, 492, 337
- Falcke, H., Melia, F., & Agol, E. 2000, *ApJ*, 528, L13
- Fendt, C. & Memola, E. 2001, *A&A*, 365, 631
- Fish, V. L., Broderick, A. E., Doeleman, S. S., & Loeb, A. 2009, *ApJ*, 692, L14
- Ghez, A. M., Salim, S., Weinberg, N. N., et al. 2008, *ApJ*, 689, 1044
- Gillessen, S., Eisenhauer, F., Trippe, S., et al. 2009, *ApJ*, 692, 1075
- Greve, A., Könönen, P., Graham, D. A., et al. 2002, *A&A*, 390, L19
- Greve, A., Torres, M., Wink, J. E., et al. 1995, *A&A*, 299, L33+
- Hawley, J. F. & Krolik, J. H. 2006, *ApJ*, 641, 103
- Hirabayashi, H., Murata, Y., Asaki, Y., et al. 2004, 5487, 1646

- Kellermann, K. I., Lister, M. L., Homan, D. C., et al. 2004, *ApJ*, *subm.*
- Keppens, R., Meliani, Z., van der Holst, B., & Casse, F. 2008, *A&A*, 486, 663
- Koide, S., Shibata, K., Kudoh, T., & Meier, D. L. 2002, *Science*, 295, 1688
- Kovalev, Y. Y., Lister, M. L., Homan, D. C., & Kellermann, K. I. 2007, *ApJ*, 668, L27
- Krichbaum, T., Graham, D., Witzel, A., Zensus, J., & et al. 2004a, in *Exploring the Cosmic Frontier: Astrophysical Instruments for the 21st Century*, 18 - 21 May 2004, Berlin, Germany, ESO Astrophysics Symposia (Springer-Verlag)
- Krichbaum, T. P. 1996, *ESO Astrophysics Symposia: Science with Large Millimetre Arrays*, p. 95, *Proceeding of the ESO-IRAM-NFRA-Onsala Workshop*, held at Garching, 11-13 December 1995, ed. P.A. Shaver, Berlin: Springer-Verlag
- Krichbaum, T. P., Agudo, I., Bach, U., Witzel, A., & Zensus, J. A. 2006a, *PoS*
- Krichbaum, T. P., Graham, D. A., Alef, W., et al. 2004b, in *European VLBI Network on New Developments in VLBI Science and Technology*, ed. R. Bachiller, F. Colomer, J.-F. Desmurs, & P. de Vicente, 15–18
- Krichbaum, T. P., Graham, D. A., Alef, W., et al. 2002, in *Proceedings of the 6th EVN Symposium*, ed. E. Ros, R. W. Porcas, A. P. Lobanov, & J. A. Zensus, 125–+
- Krichbaum, T. P., Graham, D. A., Bremer, M., et al. 2006b, *Journal of Physics Conference Series*, 54, 328
- Krichbaum, T. P., Graham, D. A., Greve, A., et al. 1997, *A&A*, 323, L17
- Krichbaum, T. P., Graham, D. A., Witzel, A., et al. 1998, *A&A*, 335, L106
- Krichbaum, T. P., Lee, S. S., Lobanov, A. P., Marscher, A. P., & Gurwell, M. A. 2008, in *Astronomical Society of the Pacific Conference Series*, Vol. 386, *Extragalactic Jets: Theory and Observation from Radio to Gamma Ray*, ed. T. A. Rector & D. S. De Young, 186–194
- Lee, S.-S., Lobanov, A. P., Krichbaum, T. P., et al. 2008, *AJ*, 136, 159
- Lobanov, A. P., Krichbaum, T. P., Graham, D. A., et al. 2000, *A&A*, 364, 391
- Ly, C., Walker, R. C., & Junor, W. 2007, *ApJ*, 660, 200
- Marscher, A. P. 1995, *Proceedings of the National Academy of Science*, 92, 11439
- . 2006, 856, 1
- McKinney, J. C. & Blandford, R. D. 2009, *MNRAS*, 394, L126
- Meier, D. L., Koide, S., & Uchida, Y. 2001, *Science*, 291, 84
- Narayan, R. 2005, *New Journal of Physics*, 7, 199
- Noble, S. C., Leung, P. K., Gammie, C. F., & Book, L. G. 2007, *Classical and Quantum Gravity*, 24, 259
- Padin, S., Woody, D. P., Hodges, M. W., et al. 1990, *ApJ*, 360, L11
- Rees, M. J., Begelman, M. C., Blandford, R. D., & Phinney, E. S. 1982, *Nature*, 295, 17
- Rogers, A. E. E., Doeleman, S., Wright, M. C. H., et al. 1994, *ApJ*, 434, L59
- Shen, Z.-Q., Lo, K. Y., Liang, M.-C., Ho, P. T. P., & Zhao, J.-H. 2005, *Nature*, 438, 62

- Tomimatsu, A., Matsuoka, T., & Takahashi, M. 2001, *Phys. Rev. D*, 64, 123003
- Tomimatsu, A. & Takahashi, M. 2003, *ApJ*, 592, 321
- Tsuboi, M. 2008, *Journal of Physics Conference Series*, 131, 012048
- Urry, C. M. & Padovani, P. 1995, *PASP*, 107, 803
- Walker, R. C., Ly, C., Junor, W., & Hardee, P. E. 2008a, *Astronomical Society of the Pacific*, 386, 87
- Walker, R. C., Ly, C., Junor, W., & Hardee, P. J. 2008b, *Journal of Physics Conference Series*, 131, 012053